

PACS numbers: 42.25.Bs, 42.25.Fx, 42.50.Gy, 42.79.Dj, 42.79.Gn, 61.05.cm, 84.40.Az

## Field Enhancement on the Dielectric-Grating Surface due to Resonant Interaction with a Plane Wave

V. Fitio, S. Holyboroda, and I. Yaremchuk

*Lviv Polytechnic National University,  
12, Stepan Bandera Str.,  
UA-79013 Lviv, Ukraine*

The power of surface Raman scattering is determined by the strength of the electromagnetic field. The field strength can be enhanced under waveguide resonance, which occurs when a plane optical wave interacts with a dielectric grating on a dielectric substrate. The resonant interaction is possible, when the optical wavelength and the grating period are carefully matched for fixed parameters of the periodic structure. Studies are carried out to determine the parameters of the grating and the parameters of the dielectric substrate, which provide significant field enhancement at the surface of the grating. The studies are performed under the normal incidence of a plane wave of TE polarization only with a wavelength of  $0.6328\ \mu\text{m}$ . The grating period is approximated based on the waveguide-mode constant propagation. The approximate grating period is always slightly smaller than the resonant grating period, greatly facilitating the search for the period, at which the reflection coefficient equals to one. The value of the refined grating period is obtained using rigorous coupled-wavelength analysis (RCWA). At this period, ‘full resonance’ is achieved. The reflection coefficient from the grating equals to one, and the field on the grating is enhanced tens or hundreds of times. As shown, the substrate does not have to be completely homogeneous with a low refractive index, but can be a combination, namely, a thin layer of a low-refractive-index dielectric deposited to the main part of a high-refractive-index substrate. As found, reducing the refractive index of the substrate and reducing the modulation of the refractive index of the grating medium lead to an increase in the fields at the grating–homogeneous medium interfaces. This method can be used to obtain a field gain of 256 times the amplitude of the incident optical wave for structures, which can be realized in practice.

Потужність поверхневого комбінаційного розсіяння визначається напруженістю електромагнетного поля. Напруженість поля може бути посиленою під час хвильового резонансу, який виникає, коли плоска оптична хвиля взаємодіє з діелектричною ґратницею на діелектричній

підкладинці. Резонансна взаємодія можлива за ретельного узгодження оптичної довжини хвилі та періоду ґратниці для фіксованих параметрів періодичної структури. Було проведено дослідження для визначення параметрів ґратниці та параметрів діелектричної підкладинки, які забезпечують значне посилення поля на поверхні ґратниці. Дослідження проводили за нормального падіння плоскої хвилі ТЕ-поляризації лише з довжиною хвилі у 0,6328 мкм. Період ґратниці був апроксимований на основі постійного поширення хвильової моди. Приблизний період ґратниці завжди трохи менший за період резонансної ґратниці, що значно полегшує пошук періоду, за якого коефіцієнт відбивання дорівнює одиниці. Значення уточненого періоду ґратниці було одержано за допомогою строгої парної аналізи довжин хвиль. У цей період досягається «повний резонанс». Коефіцієнт відбивання від ґратниці дорівнює одиниці, а поле на ґратниці посилюється в десятки та сотні разів. Показано, що підкладинка не обов'язково має бути повністю однорідною з низьким показником заломлення, але може бути комбінацією — тонкий шар діелектрика з низьким показником заломлення, нанесений на основну частину підкладинки з високим показником заломлення. Встановлено, що зменшення показника заломлення підкладинки та зменшення модуляції показника заломлення середовища ґратниці приводять до збільшення полів на межі поділу ґратниця–однорідне середовище. Цей метод можна використовувати для одержання посилення поля в 256 разів більше амплітуди падної оптичної хвилі для структур, які можна реалізувати на практиці.

**Key words:** dielectric grating, RCWA, waveguide resonance, grating reflection, field enhancement under resonance.

**Ключові слова:** діелектрична ґратниця, ретельна аналіза зв'язаних довжин хвиль, хвильовий резонанс, відбивання ґратниці, посилення поля під дією резонансу.

*(Received 18 November, 2024)*

## 1. INTRODUCTION

Combined Raman scattering is widely used to study vibrational spectra of molecules and optical vibrations of solids and liquids [1, 2]. The sample with the medium under investigation is irradiated by a light source with a narrow radiation spectrum.

There are mainly lasers, in particular He–Ne with a radiation wavelength of 632.8 nm or YAG:Nd<sup>3+</sup> with a second harmonic of 532 nm. The scattered light is shifted up or down in frequency when the laser radiation interacts with the molecules of the testing sample. The frequency shift is equal to the frequency of the oscillations occurring in the molecules, and there can be quite some such oscillation modes. A substance can be determined by frequency shifts because the molecules of each substance have only their own

vibrational modes. If the frequencies of the scattered laser radiation are shifted downward, such scattering is called Stokes scattering; if the frequency of the scattered light is shifted upward, anti-Stokes scattering is obtained [3]. The power of anti-Stokes scattering is several orders of magnitude smaller than the power of Stokes scattering.

However, even the power of Stokes radiation is quite small with limited laser power, which requires high characteristics of the optical spectrometer in terms of sensitivity and resolution. It is expected that the power of the scattered light will increase with the increase of the electromagnetic field surrounding the sample located on the substrate. A field enhancement on the substrate is possible due to the resonant interaction of the laser radiation with the substrate, which may have a complex surface structure. Surface enhanced Raman scattering (SERS) is often achieved with a nanostructured silver surface [4, 5], which is formed by electrochemical etching. The resulting signal enhancement was more than 4000 times [4]. The increase in Raman signal is explained by the increase in electromagnetic field on silver nanoparticles due to surface plasmon resonance [6].

Field enhancement methods based on resonance phenomena in periodic nanostructures are well known. There are resonances of waveguide modes by dielectric gratings on a dielectric substrate [7], resonances of surface plasmon-polariton waves by a periodic structure: a dielectric or metal grating on a metal substrate [8, 9], resonances of surface plasmons by the structure of a metal grating on a dielectric substrate [10].

However, during the resonant interaction of the electromagnetic field with structures containing metal elements, the enhanced field occurs at the metal-dielectric interface in a narrow spatial region adjacent to the metal [6, 9, 10]. Therefore, in this case, the scattered laser radiation will not be maximally possible due to the interaction in a small volume.

It should be noted that in the structure of a silver grating on a dielectric substrate, in which the resonance of surface plasmons occurs, it is possible to obtain a maximum field enhancement of several hundred times [10].

The enhanced field occurs in a significant part of the period under the resonance of waveguide modes in the structure of a dielectric grating on a metal substrate. Therefore, we have carried out a study to identify the grating parameters and the dielectric substrate parameters, which give rise to a significant field enhancement at the grating surface. The study was performed at the normal incidence of a plane wave of only TE-polarization with a wavelength of 0.6328  $\mu\text{m}$ .

## 2. RESULTS AND DISCUSSION

Precise fabrication of gratings is required to achieve waveguide resonance since the resonance response for TM-polarization is very narrow spectrally [11]. In order to identify trends in changing the parameters of the periodic structure to achieve the maximum field at the surface of the grating, the thickness of the grating was varied within sufficiently wide ranges from 300 to 1300 nm. The refractive indices of the substrate 1.457 ( $\text{SiO}_2$ ) and 1.3245 (NaF) were used. The refractive indices of the grating were  $n_{21} = 148$ ,  $n_{22} = 1.52$  and  $n_{21} = 149$ ,  $n_{22} = 1.51$ , respectively. The grating filling factor  $F = l/\Lambda = 0.5$  was the same for all numerical experiments. The numerical modelling was performed by rigorous coupled-wavelength analysis (RCWA) [12]. This makes it possible to study in detail how light propagates and interacts with materials [13].

The simplest periodic structure (a dielectric grating on a dielectric substrate) is shown in Fig. 1. It can provide a significant field at the surface of the grating ( $z = 0$ ) under waveguide resonance, and the field amplitude will be many times larger than the unit amplitude of an incident plane wave. The reflection coefficient from the grating is equal to unity with careful selection of the parameters of the periodic structure, *i.e.*, thickness and period of the grating, modulation of the refractive index of the grating medium, and the refractive index of the substrate at resonance [11]. If the refractive indices of periodic structure materials are given, then, each thickness  $d$  at waveguide resonance corresponds to a certain grating period  $\Lambda$ . The approximate period can be found using the following expression [11]:

$$2\pi/\Lambda = \beta(d, n_1, n_3, n_2), \quad (1)$$

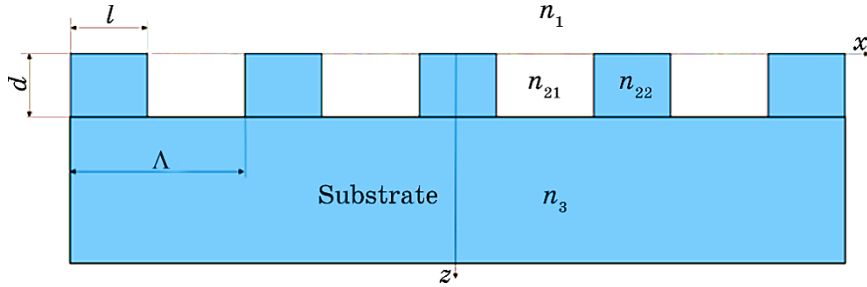


**Fig. 1.** Dielectric grating on a dielectric substrate where  $d$  is grating thickness,  $l$  is width of the part of the grating with refractive index  $n_{22}$ ,  $\Lambda$  is grating period,  $\Lambda - l$  — part of the grating with refractive index  $n_{21}$ , and  $n_{22} > n_{21}$ ,  $n_1$  and  $n_3$  are refractive indices of the surrounding medium and the substrate, respectively.

where  $\beta$  is the propagation constant of the waveguide mode of a non-symmetric waveguide that has a periodic structure.

The average value of the refractive index of the grating medium  $n_2$  is determined in the numerical analysis as follows:

$$n_2 = \sqrt{\frac{n_{21}^2 + n_{22}^2}{2}}. \quad (2)$$

If  $n_{22} - n_{21} \rightarrow 0$ , then,  $\Lambda$  calculated by Eq. (1) goes to the period, in which the reflection coefficient is unity. Having the value of  $\Lambda$  according to Eq. (1), and this value is very close to the resonance value, we find  $\Lambda$  that ensures the reflection coefficient  $R > 0.9999$ . after several steps of numerical analysis. It should be noted that the grating period calculated by Eq. (1) is always slightly smaller than the resonance period of the grating. It greatly facilitates the search for the period, at which the reflection coefficient is equal to unity. The approximate and exact values of  $t$  period for different thicknesses and different  $n_3$ ,  $n_{21}$ ,  $n_{22}$  are given in Table. It is possible to judge the accuracy of the analysis according to Eq. (1) from this Table.

The propagation constants of the waveguide modes  $\beta$  have been determined by the method described in [12], which ensures precise accuracy [14]. It should be noted that this method is suitable for the analysis of gradient planar waveguides and all discrete propagation constants and corresponding field distributions in the waveguide can be found in one calculation cycle.

The field distributions in the waveguide with a grating thickness of 500 nm for  $n_{21} = 1.49$ ,  $n_{22} = 1.51$  and for two values of  $n_3$  are shown in Fig. 2.

The field distribution, corresponding the power of the waveguide mode propagating along the waveguide, is more concentrated in the layer with refractive index  $n_2$ , when  $n_3 = 1.3245$ , as shown in Fig. 2. Therefore, it can be expected that a stronger field can be obtained under waveguide resonance on the grating surface ( $z = 0$ ) for  $n_3 = 1.3245$ . The magnitude of the field at the grating surface can be predicted using the following expression:

$$K = \frac{|E(0)|}{|E(d)|}. \quad (3)$$

As a result, we obtain  $K = 0.321$  at  $n_3 = 1.457$  and  $K = 0.632$  at  $n_3 = 1.3245$ . This means that the  $K$ -ratio is about twice as high at  $n_3 = 1.3245$  compared to  $n_3 = 1.457$ . These preliminary findings confirm the calculated results of the fields at the grating surface and the grating/substrate interface using RCWA. The corresponding field distribution is shown in Fig. 3 for the same structure pa-

**TABLE.** Resonance parameters for the periodic structure.

$d, \mu\text{m}$	$\beta, \mu\text{m}^{-1}$	$\Lambda_{pr}, \mu\text{m}$	$\Lambda, \mu\text{m}$	$ E(0, 0) $	$ E(0, d) $
$n_3 = 1.3245, n_{21} = 1.49, n_{22} = 1.51$					
0.6	14.419938	0.435729	0.435756	95	153
<b>0.5</b>	<b>14.286058</b>	<b>0.439812</b>	<b>0.439840</b>	<b>265</b>	<b>419</b>
0.4	14.090589	0.445914	0.445943	83	130
0.3	13.798510	0.455352	0.455377	55	89
$n_3 = 1.457, n_{21} = 1.48, n_{22} = 1.52$					
<b>1.3</b>	<b>14.778269</b>	<b>0.425164</b>	<b>0.425275</b>	<b>58</b>	<b>175</b>
1.0	14.724143	0.426727	0.426831	27	90
0.9	14.698037	0.427485	0.427588	49	150
0.8	14.666097	0.428416	0.428518	25	77
0.7	14.627004	0.429561	0.429655	19	64
0.6	14.579813	0.430951	0.431029	27	90
0.5	14.525943	0.432549	0.432611	36	112
<b>0.435</b>	<b>14.491739</b>	<b>0.433570</b>	<b>0.433615</b>	<b>54</b>	<b>163</b>
0.4	14.476808	0.434017	0.434048	34	105
$n_3 = 1.457, n_{21} = 1.49, n_{22} = 1.51$					
<b>1.3</b>	<b>14.77732</b>	<b>0.425191</b>	<b>0.425219</b>	<b>113</b>	<b>350</b>
0.9	14.697162	0.427510	0.427536	97	301
0.8	14.665265	0.428440	0.428465	49	153
0.7	14.626232	0.429583	0.429606	39	127
0.6	14.579137	0.430971	0.430990	55	179
<b>0.5</b>	<b>14.525426</b>	<b>0.432564</b>	<b>0.432579</b>	<b>72</b>	<b>224</b>
<b>0.435</b>	<b>14.491388</b>	<b>0.433581</b>	<b>0.433591</b>	<b>106</b>	<b>325</b>
0.4	14.476580	0.4340244	0.434031	68	209

rameters as in Fig. 2. It can be seen that the field with the magnitude  $|E(x)| > |E(0)|/2$  occupies most of the grating period, which is important for SERS. In addition, a decrease in the refractive index of the substrate leads to a significant increase in the fields under other identical conditions.

It should be noted that it is unnecessary to make the substrate with a low refractive index completely homogeneous. It is possible to make a combined one: a thin layer of dielectric with low refractive index applied on the main part of the substrate with high refractive index. The layer thickness of 1000 nm with a low refractive index of 1.3245 is sufficient as shown in Fig. 2, *b*.

The grating periods  $\Lambda_{pr}$  calculated with Eq. (1) and the refined periods  $\Lambda$  determined with RCWA, as well as the fields at  $x = 0$  for  $z = 0$   $|E(0, 0)|$  and for  $z = d$   $|E(0, d)|$  are presented in Table. Calcula-

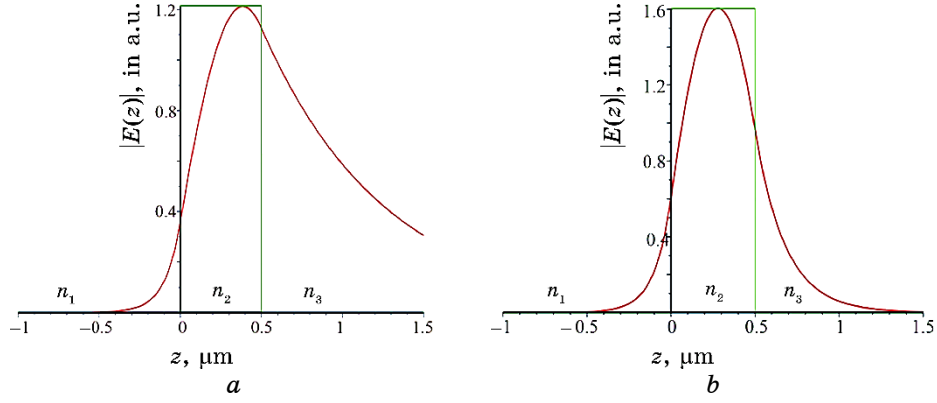


**Fig. 2.** Field distribution in a periodic structure (red curves), as in a planar waveguide, with  $n_1=1$  and with  $n_3=1.457$  (a), and with  $n_3=1.3245$  (b). The green lines define the boundaries of the grating.

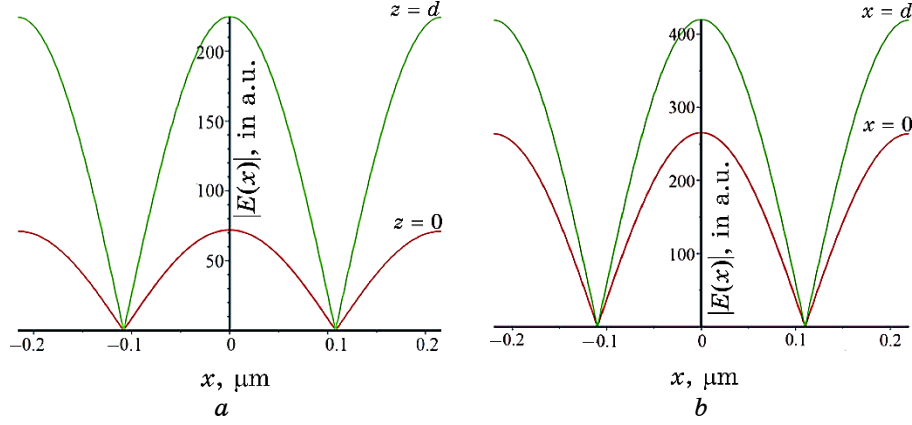


**Fig. 3.** Field distribution in the periodic structure along the grating period at  $n_1=1$ , the grating thickness of 500 nm and  $n_3=1.457$  (a), and  $n_3=1.3245$  (b).

tions, which are more detailed, have been made for the parameters in bold in the table, and the results are shown in Figs. 3, 4 and 5.

As shown in Table, the strongest fields on the grating surface and at the grating/substrate interface are obtained with a smaller modulation of the refractive index ( $n_{21}=1.49$ ,  $n_{22}=1.51$ ) and for the substrate refractive index of 1.3245. At the same time, the optimal grating thickness  $d$  is of 500 nm. As a result,  $|E(0,0)|=265$ , under the condition that the amplitude of the incident grating wave is unity, *i.e.*, we have a 265-fold field enhancement under resonance.

Spectral dependences of the reflection coefficient and spectral de-

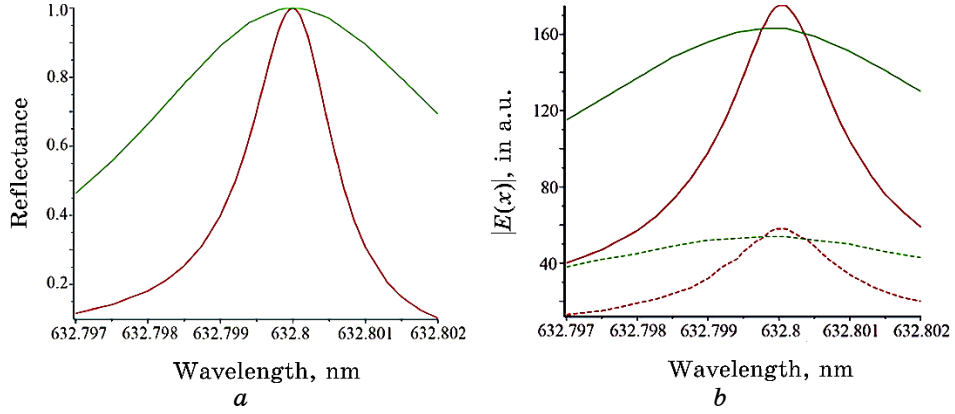


**Fig. 4.** Spectral dependences of the reflection coefficient (a) and the fields on the grating surface (dashed curves) and at the grating/substrate interface (solid curves) (b). The red colour of the curves corresponds to parameters  $d = 1300$  nm,  $n_3 = 1.457$ ,  $n_{21} = 1.48$ ,  $n_{22} = 1.52$ ; the green colour of the curves corresponds to parameters  $d = 435$  nm,  $n_3 = 1.457$ ,  $n_{21} = 1.48$ ,  $n_{22} = 1.52$ .

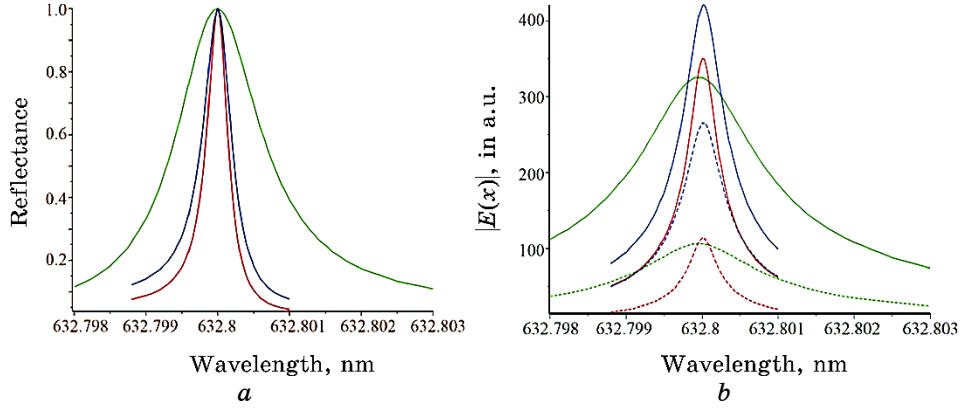


**Fig. 5.** Spectral dependences of the reflection coefficient (a) and the fields on the grating surface (dashed curves) and at the grating/substrate interface (solid curves) (b). The red colour of the curves corresponds to parameters  $d = 1300$  nm,  $n_3 = 1.457$ ,  $n_{21} = 1.49$ ,  $n_{22} = 1.51$ ; the green colour of the curves corresponds to parameters  $d = 500$  nm,  $n_3 = 1.3245$ ,  $n_{21} = 1.49$ ,  $n_{22} = 1.51$ .

pendences of the field amplitude module for  $z = 0$  and  $z = d$  at  $x = 0$  are shown in Figs. 4 and 5, respectively.

As can be seen from the comparison of Fig. 4 and Fig. 5, the width of the spectral response of both the reflection coefficient of



the grating and the modulus of the field amplitude decreases as the modulation of the refractive index of the grating medium is reduced. We can also see that the resonance widths at half the response height are quite narrow, about nm, which requires precision fabrication of such gratings. However, it is quite possible to fabricate such periodic structures by recording holograms on photopolymer compositions [15, 16] with a modulation amplitude of the refractive index of the photopolymer composition of 0.017 [15].

### 3. CONCLUSIONS

Significant field enhancement of 256 times can be obtained at the air-grating interface with an optimal choice of the grating thickness and other parameters of the structure in the periodic structure of type the dielectric grating on the dielectric substrate under the waveguide resonance. Numerical studies have shown that the field on the grating increases as the refractive index of the substrate decreases and as the modulation of the refractive index of the grating medium decreases. The resonant period of the grating can be approximated by the propagation constant of the waveguide mode in a periodic structure such as a waveguide for the given wavelength. The exact value of the grating resonance period can be determined using RCWA. It should be noted that the period of the grating calculated by Eq. (1) is always slightly smaller than the resonant period of the grating. It greatly facilitates the search for the period at which the reflection coefficient is equal to one.

### ACKNOWLEDGMENT

The authors acknowledge the financial support of this research by the Ministry of Education and Science of Ukraine with the DB/SERS project (state registration number 0124U000823).

### REFERENCES

1. J. Langer, D. Jimenez de Aberasturi, J. Aizpurua, R. A. Alvarez-Puebla, B. Augu  , J. J. Baumberg, and L. M. Liz-Marz  n, *ACS Nano*, **14**, No. 1: (2019); <https://doi.org/10.1021/acsnano.9b04224>
2. W. Wang, P. Ma, and D. Song, *Luminescence*, **37**: 1822 (2022); <https://doi.org/10.1002/bio.4383>
3. A. Yariv, *Quantum Electronics* (New York–London–Sydney–Toronto: John Wiley and Sons, Inc.–California Institute of Technology: 1975).
4. Ch. H. Lee, T. Limei, and S. Singamaneni, *ACS Appl. Mater. Interfaces*, **2**: 3429 (2010); <https://doi.org/10.1021/am1009875>
5. S. Nie and S. R. Emory, *Science*, **275**: 1102 (1997);

- doi:[10.1126/science.275.5303.1102](https://doi.org/10.1126/science.275.5303.1102)
6. R. Wang, J. Ma, X. Dai, Y. Gao, C. Gu, and T. Jiang, *Sensors and Actuators B: Chemical*, **374**: 132782 (2023); <https://doi.org/10.1016/j.snb.2022.132782>
7. G. Quaranta, G. Basset, O. J. F. Martin, and B. Gallinet, *Laser Photonics Rev.*, **12**: 1800017 (2018); <https://doi.org/10.1002/lpor.201800017>
8. S. Bellucci, O. Vernyhor, A. Bendziak, I. Yaremchuk, V. Fitio, and Y. Bobitski, *Materials*, **13**: 1882 (2020); <https://doi.org/10.3390/ma13081882>
9. V. M. Fitio and Y. V. Bobitski, *J. Opt. A: Pure Appl. Opt.*, **6**: 943 (2004); doi:[10.1088/1464-4258/6/10/004](https://doi.org/10.1088/1464-4258/6/10/004)
10. V. Fitio, I. Yaremchuk, O. Vernyhor, and Ya. Bobitski, *Applied Nanoscience*, **8**: 1015 (2018); <https://doi.org/10.1007/s13204-018-0686-z>
11. S. S. Wang and R. Magnusson, *Appl. Opt.*, **32**: 2606 (1993); <https://doi.org/10.1364/AO.32.002606>
12. V. M. Fitio, V. V. Romakh, and Y. V. Bobitski, *Semiconductor Physics, Quantum Electronics & Optoelectronics*, **19**: 28 (2016); doi:[10.15407/spqeo19.01.028](https://doi.org/10.15407/spqeo19.01.028)
13. B. J. Civiletti, A. Lakhtakia, and P. B. Monk, *Journal of Computational and Applied Mathematics*, **368**: 112478 (2020); <https://doi.org/10.1016/j.cam.2019.112478>
14. V. M. Fitio, V. V. Romakh, L. V. Bartkiv, and Y. V. Bobitski, *Materials Science & Engineering Technology* [Materialwissenschaft und Werkstofftechnik], **47**: 237 (2016); <https://doi.org/10.1002/mawe.201600473>
15. T. Smirnova, V. Fitio, O. Sakhno, P. Yezhov, A. Bendziak, V. Hryn, and S. Bellucci, *Nanomaterials*, **10**: 2114 (2020); <https://doi.org/10.3390/nano10112114>
16. G. M. Karpov, V. V. Obukhovskiy, T. N. Smirnova, and V. V. Lemesenko, *Opt. Commun.*, **174**: 391 (2000); doi:[10.1016/S0030-4018\(99\)00712-9](https://doi.org/10.1016/S0030-4018(99)00712-9)